ELSEVIER

Carbohydrate Polymers 52 (2003) 243–252

Carbohydrate Polymers

www.elsevier.com/locate/carbpol

Constitutive modeling of β-glucan/amylodextrin blends☆

Jeffrey A. Byars*, Craig J. Carriere, George E. Inglett

Cereal Products and Food Science Research Unit, National Center for Agricultural Utilization Research, Agricultural Research Service, United States Department of Agriculture, 1815 N University Street, Peoria, IL 61604, USA

Received 24 January 2002; revised 2 October 2002; accepted 3 October 2002

Abstract

Accurate constitutive equations are required for the understanding of many food processes. The purpose of this work was to test the ability of constitutive equations to model the rheological behavior of β-glucan/amylodextrin blends in a range of flows. The predictions of the K-BKZ, Giesekus, Phan-Thien–Tanner and Bird–Carreau models were compared to experimental results in steady shear, startup of steady shear, stress relaxation and biaxial extension flows. The K-BKZ model yielded the most accurate predictions across the range of flows. The Giesekus and Phan-Thien–Tanner models gave good results in shear flows, but failed to predict the correct strain dependence in stress relaxation. The Bird–Carreau model did not capture many features of the flow behavior. The results indicate the need to test thoroughly constitutive equations before using them to model food processes.
Published by Elsevier Science Ltd.

Keywords: Rheology; Constitutive modeling; β-Glucan/amylodextrin blends

1. Introduction

Understanding the rheological and flow behavior of biopolymers is important both in setting processing conditions and in studying the textural properties of a finished product. Constitutive equations aid in the understanding of flow behavior, since they provide an important link between fundamental rheological properties and more complex flow phenomena. While many constitutive equations have been developed and tested for synthetic polymers (Bird, Armstrong, & Hassager, 1987; Larson, 1988), only limited information regarding their applicability to biopolymers is available.

This work studies the flow behavior and constitutive modeling of Oatrim suspensions. Oatrim is a blend of amylodextrins and β-glucan prepared from an enzymatic conversion of oat bran (Inglett, 1993). Because soluble oat fibers have important health benefits by reducing blood cholesterol (Food and Drug Administration, 1997a,b), many authors have investigated the solution behavior of oat β-glucans. Previous studies (Zhang, Doehlert, & Moore, 1998; Doublier & Wood, 1995; Wikström, Lindahl, Andersson, & Westerlund, 1994; Autio, Myllymäki, & Mälkki, 1987) have shown that aqueous solutions of β-glucan are shear-thinning, and that their behavior in oscillatory flow is characteristic of entangled polymer solutions. Carriere and Inglett (1998, 1999) have also studied Oatrim suspensions. A region of shear-thickening in the viscosity of Oatrim suspensions was observed. The shear-thickening was attributed to interactions between the β-glucans and amylodextrins that comprise Oatrim. However, none of these studies has investigated the ability of constitutive equations to model the flow behavior of the β-glucan or Oatrim solutions.

In order to assess the accuracy of a constitutive model in predicting flow behavior, it is necessary to obtain values for the model's parameters from well-defined flows, and then compare the model's predictions to experimental results in other well-defined flows. Carriere, Thomas and Inglett (2002) used the K-BKZ model to study the flow behavior of flour suspensions. The model yielded accurate predictions in steady shear flow and startup of steady shear flow for suspensions of defatted oat flour, barley flour and oat bran, while predictions for oat flour suspensions were less

☆ Names are necessary to report factually on available data; however, the USDA neither guarantees nor warrants the standard of the product, and the use of the name by the USDA implies no approval of the product to the exclusion of others that may also be suitable.

* Corresponding author. Tel.: +1-309-681-6330; fax: +1-309-681-6685.
E-mail address: byarsja@ncaur.usda.gov (J.A. Byars).

0144-8617/03/$ - see front matter Published by Elsevier Science Ltd.
PII: S0144-8617(02)00272-2

accurate. Dhanasekharan, Huang and Kokini (1999) and Dhanasekharan, Wang and Kokini (2001) compared the predictions of differential constitutive models to the measured rheology of different doughs. They found that the White–Metzner model gave more accurate predictions than the Giesekus or Phan-Thien–Tanner models, although none of the models was accurate in all of the flows considered.

The goal of the current work is to measure the rheology of Oatrim suspensions in a wide range of flows, and to study the ability of four different constitutive equations to predict the observed flow behavior. Results are presented below for the rheology of Oatrim suspensions in small amplitude oscillatory shear flow, steady shear, startup of steady shear, stress relaxation and biaxial extension flows. These results are compared to the predictions of the Giesekus, Phan-Thien–Tanner, K-BKZ and Bird–Carreau models.

2. Materials and methods

2.1. Sample preparation

The preparation of Oatrim has been described by Inglett (1993). Briefly, an oat bran slurry was passed through a steam jet cooker and collected in a heated kettle. An α-amylase was added to the slurry and held at 85–90 °C for 5 min. The slurry was then passed through the jet cooker again to deactivate the enzyme. The soluble fraction was separated by centrifugation and freeze-dried to yield Oatrim. The suffix for each preparation indicates the weight percent of β-glucan. Oatrim-5 contained 86 wt% amylodextrins, while Oatrim-10 had 81 wt%. Each also contained 4 wt% ash, 4 wt% protein and 1 wt% crude fat.

Oatrim suspensions were prepared by mixing the Oatrim powder in deionized water with a Janke and Kunkel Ultra-Turrax T25 disperser (IKA Labortechnik, Staufen, Germany). Some viscous heating occurred during mixing, and samples were allowed to cool to room temperature before testing. Air was entrained in the samples during mixing, and it was removed either by letting the sample stand or by applying a vacuum for more viscous samples. For the biaxial extension tests, gels were formed by pouring sample into steel bushings which served as molds. The internal diameter was 38.1 mm, and heights from 1.1 to 3.0 mm were used. The bushings were placed between lubricated glass plates and allowed to stand at room temperature for 24 h before testing.

2.2. Rheological measurements

Measurements in small amplitude oscillatory shear, steady shear, startup of steady shear and stress relaxation flows (Bird et al., 1987) were conducted on a Rheometrics ARES (Piscataway, NJ) controlled strain fluids rheometer. Tests were performed with 50 mm diameter parallel plates. For the relaxation experiments, the deformation was imposed within 0.08 s for all strains. A circulating water bath was used to maintain the temperature at 25.0 ± 0.1 °C, and humidity covers were used to prevent drying of the samples. The errors of the rheological measurements were within 10% of the mean values reported.

Biaxial extension experiments were conducted with a Texture Technologies (Scarsdale, NY) TA-XT2i texture analyzer. The upper fixture was a 101.6 mm diameter disk, and a flat plate was used as the bottom surface. The surfaces were parallel to within 0.05°. Both surfaces were covered with a sheet of teflon, and a coating of vegetable oil was applied to each surface to ensure that the Oatrim sample would not stick. The gap between the surfaces was zeroed, the upper disk was raised to a known height, and the sample was placed on the lower surface. The upper plate was then lowered at a constant speed, and the force was recorded as a function of height. Assuming that slip occurs at the plate, this will generate a biaxial extensional flow (Soskey & Winter, 1985; Chatraei & Macosko, 1981). The strain rate, $\dot{\epsilon}(t)$, is given by

$$\dot{\epsilon}(t) = -\frac{v}{h(t)}, \tag{1}$$

where v is the velocity of the upper disk and $h(t)$ is the sample height. The normal stress difference is calculated from the force reading and the instantaneous sample radius. The sample radius remained less than the radius of the upper plate for all tests reported here. Since the upper plate is not in contact with the sample at the beginning of the test, it was necessary to ensure that the sample was of uniform thickness so that the moving plate would contact the entire sample at the same time.

2.3. Constitutive modeling

The primary goal of this work was to evaluate the ability of commonly used constitutive equations to predict accurately the flow behavior of Oatrim suspensions and gels. The following four equations were selected since they have been used previously for modeling the rheology of food and biopolymer systems (Kokini, 1994; Bagley, 1992; Carriere et al., 2002). The same linear viscoelastic spectrum $\{\lambda_i, \eta_i\}$ with six modes was used for the Giesekus, Phan-Thien–Tanner and K-BKZ models. The relaxation time, λ_i, and viscosity, η_i, for each mode were determined from a fit of a multimode Maxwell model to small amplitude oscillatory shear flow and small strain stress relaxation data.

$$G'(\omega) = \sum_i \frac{\eta_i \lambda_i \omega^2}{1 + (\lambda_i \omega)^2} \tag{2}$$

$$G''(\omega) = \sum_i \frac{\eta_i \omega}{1 + (\lambda_i \omega)^2} \tag{3}$$

$$G(t) = \sum_i \frac{\eta_i}{\lambda_i} \exp(-t/\lambda_i) \quad (4)$$

2.3.1. Giesekus model

The Giesekus model (Giesekus, 1982) is based on reptation theory, and assumes that a Hookean dumbbell can translate more easily along the direction of its backbone than normal to it. The anisotropic mobility coefficient, α, describes the extent of nonlinearity:

$$\tau_i + \lambda_i \tau_{i(1)} - \frac{\alpha_i \lambda_i}{\eta_i}(\tau_i \cdot \tau_i) = -\eta_i \dot{\gamma} \quad (5)$$

where τ_i is the extra stress tensor for each mode, $\tau = \sum \tau_i$ is the extra stress tensor, and $\dot{\gamma}$ is the rate-of-strain tensor. The α_i were obtained by fitting the viscosity as a function of shear rate. The mobility coefficient determines not only the shear rate dependence of the viscosity, but also the steady-state value of the extensional viscosity.

2.3.2. Phan-Thien–Tanner (PTT) model

The Phan-Thien–Tanner model (Phan-Thien & Tanner, 1977; Phan-Thein, 1978) is derived from network theory, and network junctions are assumed to slip relative to the bulk deformation. The parameter ξ_i describes the extent of the nonaffine deformation. The rate of creation (and destruction) of network junctions is governed by the parameter ϵ_i.

$$Z(\mathrm{tr}\tau_i)\tau_i + \lambda_i \tau_{i(1)} + \frac{\xi_i}{2}\lambda_i(\dot{\gamma}\cdot\tau_i + \dot{\gamma}\cdot\tau_i) = -\eta_i \dot{\gamma} \quad (6)$$

where

$$Z(\mathrm{tr}\tau_i) = 1 - \frac{\epsilon_i \lambda_i}{\eta_i}\mathrm{tr}\tau_i \quad (7)$$

or

$$Z(\mathrm{tr}\tau_i) = \exp\left(-\frac{\epsilon_i \lambda_i}{\eta_i}\mathrm{tr}\tau_i\right). \quad (8)$$

The ξ_i were obtained by fitting the viscosity as a function of shear rate, assuming that $\epsilon_i = 0$. The ϵ_i mainly influence extensional flow properties, and were not determined.

2.3.3. K-BKZ model

The K-BKZ model (Kaye, 1962; Bernstein, Kearsley, & Zapas, 1963) is an empirical equation that assumes that the time and strain dependence of the stress are separable:

$$\tau(t) = \int_{-\infty}^{t'} m(t-t')h(\gamma)\mathbf{B}(t,t')\mathrm{d}t', \quad (9)$$

where $m(t-t')$ is the memory function,

$$m(t-t') = \sum_i \frac{\eta_i}{\lambda_i^2}\exp[-(t-t')/\lambda_i], \quad (10)$$

$h(\gamma) = K\mathrm{e}^{-a_1\gamma} + (1-K)\mathrm{e}^{-a_2\gamma}$ is the damping function as a function of the strain, γ, and $\mathbf{B}(t,t')$ is the Finger strain tensor, which describes the deformation applied to the sample.

2.3.4. Bird–Carreau model

The Bird–Carreau model (Bird & Carreau, 1968; Carreau, MacDonald, & Bird, 1968) is given by:

$$\tau(t) = -\int_{-\infty}^{t}\sum_{k=1}^{\infty}\frac{\eta_k}{\lambda_k^{(2)^2}}\frac{\mathrm{e}^{-(t-t')/\lambda_k^{(2)}}}{1+(\lambda_k^{(1)}\dot{\gamma}(t'))^2}\mathbf{B}(t,t')\mathrm{d}t' \quad (11)$$

where

$$\eta_k = \eta_0\frac{\lambda_k^{(1)}}{\sum_{k=1}^{\infty}\lambda_k^{(1)}} \quad (12)$$

$$\lambda_k^{(n)} = \lambda_n\left(\frac{2}{k+1}\right)^{\alpha_n} \quad (13)$$

The value of η_0 was taken to be $\eta_0 = \sum\eta_i$, using the η_i obtained from the linear viscoelastic spectrum. The values of λ_1 and α_1 can be determined graphically from the shear rate dependence of the viscosity, while λ_2 and α_2 can be determined from the frequency dependence of the dynamic viscosity (Kokini, 1994). The summations in Eq. (12) were well-approximated by the first 100 terms for the calculations.

Fits of the linear viscoelastic spectra and nonlinear parameters of the differential models were obtained using a quasi-Newton algorithm with MathCad software (MathSoft, Cambridge, MA). The differential constitutive equations were solved with an adaptive step size control Runge–Kutta method, and the integral constitutive equations were solved with an adaptive quadrature algorithm.

3. Results and discussion

The effect of concentration on the small amplitude oscillatory shear flow properties of Oatrim-10 suspensions is shown in Fig. 1. The storage modulus, G', is shown as a function of frequency for concentrations between 4 and 16% by weight (all concentrations are on a dry weight basis). As the concentration increases, the value of the storage modulus increases, and its frequency dependence becomes weaker. Although not shown for clarity, the loss modulus, G'', increases in a similar manner with concentration. However, G'' does not increase as sharply with concentration as G' does, resulting in a more elastic fluid at higher concentrations. This is indicated in Fig. 1(b), which shows $\tan\delta \equiv G''/G'$ at a frequency of 1 rad/s as a function of concentration. $\tan\delta$ decreases by almost an order of magnitude as the concentration is increased from 6 to 16 wt%. At the highest concentrations, $\tan\delta < 1$, indicating that elastic effects are dominant. Although $\tan\delta$ was not constant with frequency, a similar trend was observed at other frequencies. For concentrations of 12 wt% or greater,

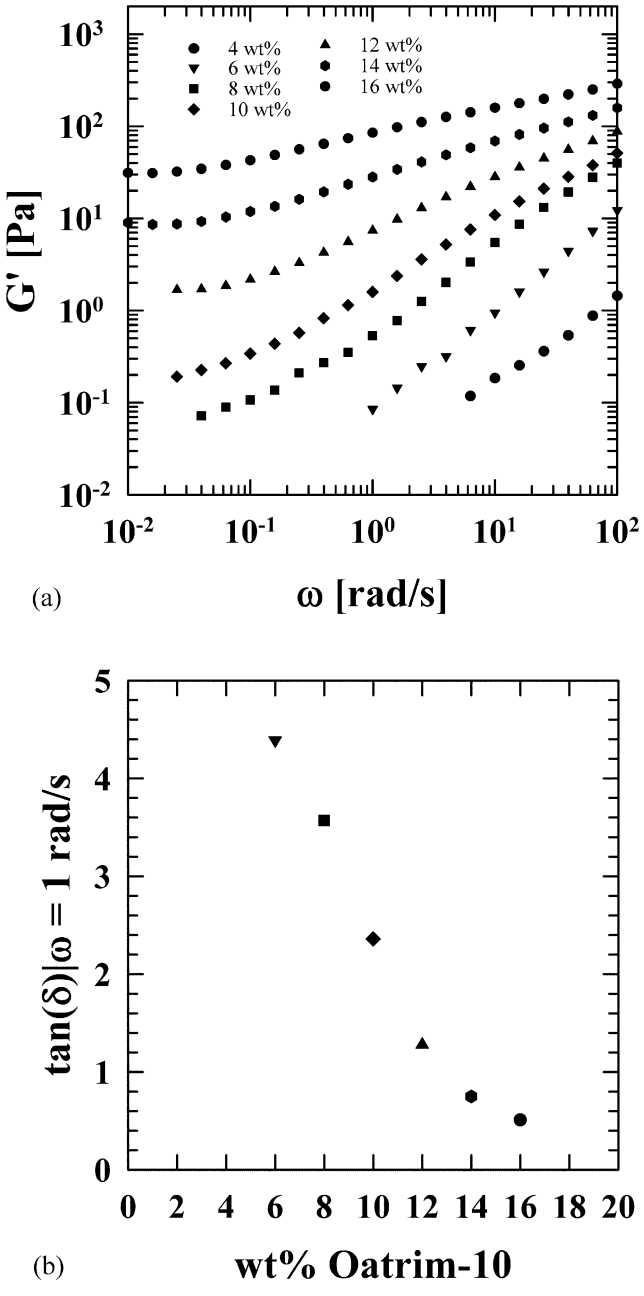

Fig. 1. Concentration dependence of small amplitude oscillatory shear flow properties of Oatrim-10 solutions. (a) Storage modulus; (b) loss tangent at a frequency of 1 rad/s.

tan δ varied by less than 50% over the range of frequencies studied, while for lower frequencies tan δ decreased with frequency. At the highest concentrations, the weak gel began to slip in steady shear flow and startup of steady shear flow. Because the goal of this paper is to test the ability of constitutive models to predict flow behavior in as wide a range of flows as possible, most of the results presented here are for the 12 wt% Oatrim-10 suspension. Additional results are presented for a 20 wt% Oatrim-5 suspension that forms a gel stronger than the 16 wt% Oatrim-10 sample.

The linear viscoelastic spectrum $\{\lambda_i, \eta_i\}$ was determined from a combination of the small amplitude oscillatory shear flow data and stress relaxation data at low strain. The same set of $\{\lambda_i, \eta_i\}$ should fit the results of each experiment, so a fit was obtained to minimize the total error, with equal weight given to the frequency sweep and stress relaxation experiments. This combined fit extends the range of time constants that can be determined, since the frequency sweep will be characterized by time constants that are the inverse of the frequency range studied ($\lambda = 0.01-30$ s), whereas the stress relaxation will be characterized by time constants that depend on the length of the experiment ($\lambda = 0.1-100$ s). The small amplitude oscillatory shear data were used to determine the parameters α_2 and λ_2 in the Bird–Carreau model following the graphical procedure described by Kokini (1994).

There are many possible solutions to Eqs. (2–4), and many methods for obtaining these solutions (Malkin & Masalova, 2001). In this case, the six relaxation modes $\lambda_i = 10^{-2}, 10^{-1}, \ldots, 10^{3}$ were fixed and the η_i were determined to minimize the error in Eqs. (2–4). Fig. 2 shows that six modes are sufficient to obtain a good fit to the data for the entire range of frequency and time studied. The values for the linear viscoelastic spectrum are given in Table 1.

The viscosity as a function of shear rate, along with the fit for each model, is shown in Fig. 3. The shear-thickening of the viscosity near $\dot{\gamma} = 30\ s^{-1}$ is typical of Oatrim suspensions. This effect has been described in detail by Carriere and Inglett (1999), who attributed it to interactions between the β-glucans and amylodextrins. For the Giesekus and PTT models, the nonlinear parameters, α_i and ξ_i, respectively, were determined in order to give the best fit to the viscosity data. The experimental results were also used to determine graphically the parameters α_1 and λ_1 in the Bird–Carreau model. Each of these models is able to fit accurately the measured data over the range of shear rates studied, but the Giesekus model was the only model to fit the shear-thickening region. The nonlinear parameters for each model are also given in Table 1. The very high values (>0.85 for most modes) for α_i and ξ_i for the Giesekus and PTT models, respectively, are atypical. They indicate that the linear viscoelastic spectrum tends to overpredict the viscosity measurements, as a high value of the nonlinear parameter has the effect in Fig. 3 of causing shear-thinning of the viscosity to occur at a lower shear rate. Nevertheless, with six relaxation modes, the viscosity data can be fitted well by these models. Whereas the viscosity data was used to obtain the model parameters for the above models, the results for the K-BKZ model are the prediction of the model, using the damping function determined from the stress relaxation experiments discussed below. This model underpredicts the viscosity at all shear rates, although it is much closer to the measured values at high shear rates, and the correct slope is predicted at high shear rates. However, the onset of shear-thinning is predicted to occur at a much lower shear rate

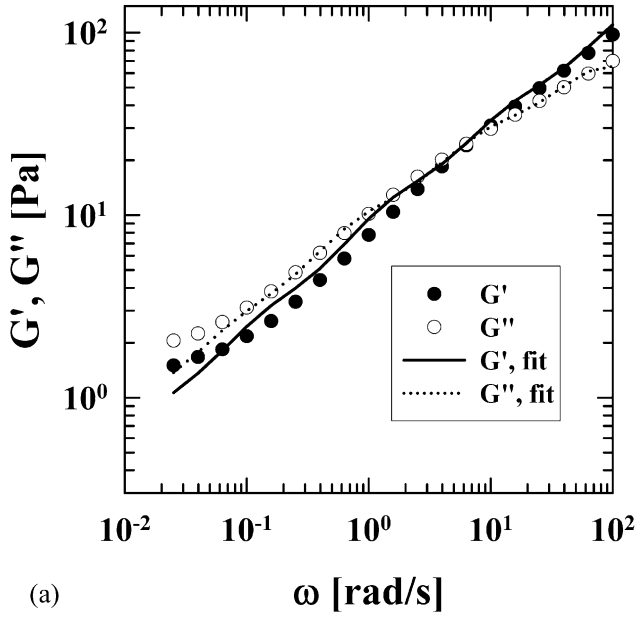

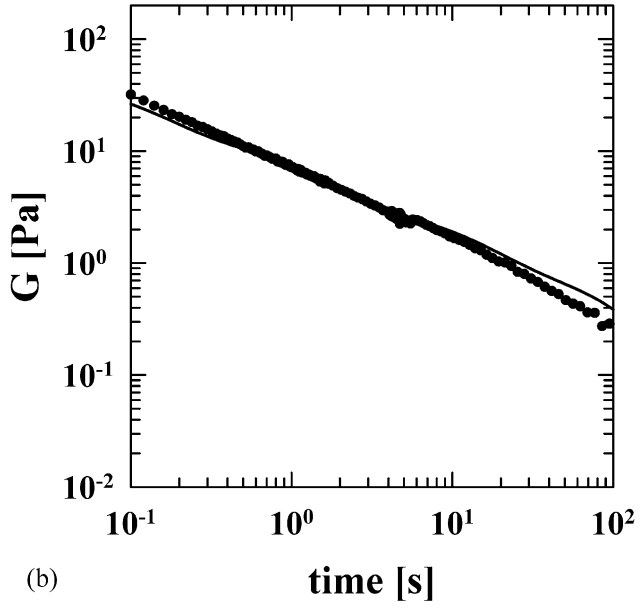

Fig. 2. Linear viscoelastic properties of 12 wt% Oatrim-10. The curves are the fit of a six-mode Maxwell model. (a) Small amplitude oscillatory shear flow; (b) relaxation modulus at $\gamma = 0.05$.

than is experimentally observed, so the model underpredicts the viscosity by almost 70% at low shear rates.

The results in Figs. 2 and 3 (and Fig. 6 below for the K-BKZ model) have been used to determine the linear viscoelastic spectrum and the nonlinear parameters of the models. The results below test the predictions of the constitutive equations using these parameters in more complex, although still well-defined, flows. The transient response of each model is shown in Figs. 4 and 5, for the startup of steady shear at shear rates of 0.1 and 10 s^{-1}, where $\eta^+(t;\dot{\gamma}) = \tau(t)/\dot{\gamma}$. At $\dot{\gamma} = 0.1\ s^{-1}$, the viscosity increases for about 10 s, and then decays slowly to its steady value. Because of variations between samples, the final value in Fig. 4 does not agree exactly with the value in Fig. 3; however, the qualitative features of the startup behavior were the same for all samples. Both the Giesekus and PTT models predict an overshoot on startup that is similar to the experimental value. The time at which the predicted maximum occurs is longer than for the measured values, and the decrease from the maximum is quicker than observed. The PTT model then undershoots and has a second overshoot before reaching its final value. As expected from Fig. 3, the predicted values for the K-BKZ model are well below the measured value. It predicts a maximum on startup to occur at about the same time as measured, although with a much smaller magnitude. The Bird–Carreau model does not predict any overshoot in the viscosity, and it takes longer to reach a steady value than experimentally observed. The absence of an overshoot on startup of steady shear flow is a general feature of the Bird–Carreau model (Yamamoto, 1971; van Es & Christensen, 1973), and is not dependent on the parameters obtained from fitting the data in Figs. 2 and 3. Although there are cases

Table 1
Model parameters for the 12 wt% Oatrim-10 sample

	λ_i (s)	η_i (Pa s)	Giesekus α_i	PTT ξ_i	K-BKZ		Bird–Carreau	
					K	a_i	λ_i (s)	α_i
1	0.01	1.24	0.904	0.999	0.462	0.058	52.5	2.87
2	0.1	3.43	0.998	0.999		0.0099	564	4.29
3	1	11.18	0.998	0.999				
4	10	26.11	0.998	0.156				
5	100	104.7	0.165	0.045				
6	1000	0.50	0.899	0.857				

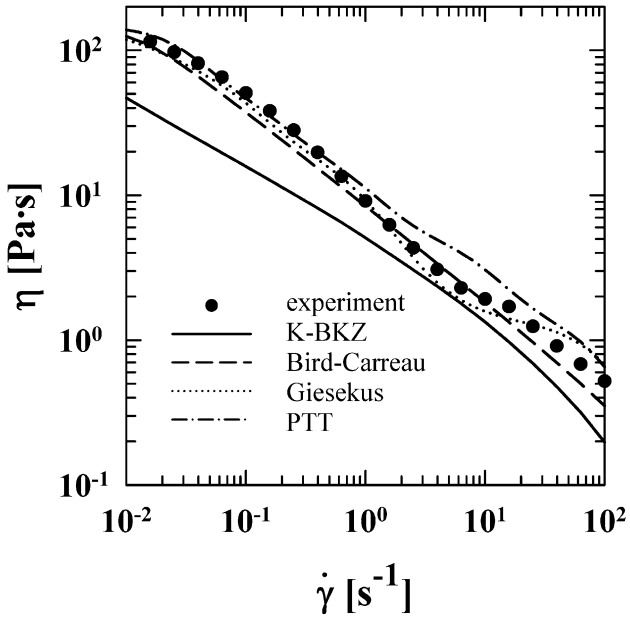

Fig. 3. Viscosity of 12 wt% Oatrim-10.

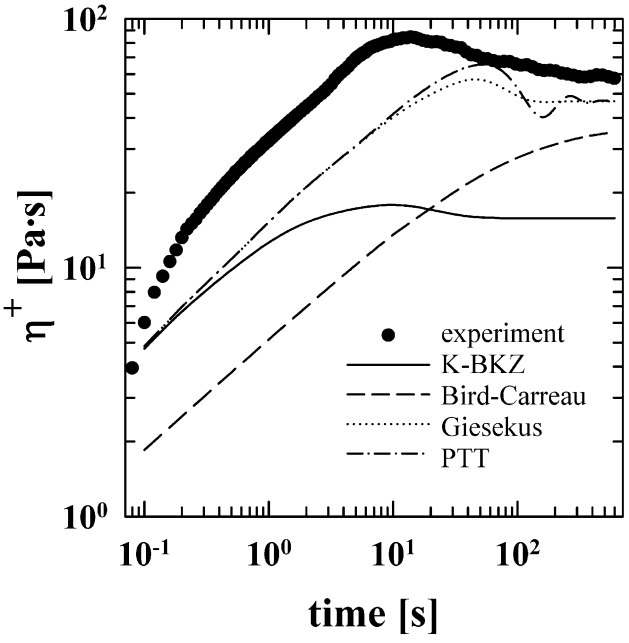

Fig. 4. Startup of steady shear flow of 12 wt% Oatrim-10 at $\dot{\gamma} = 0.1\ s^{-1}$.

where an overshoot can be predicted by the Bird–Carreau model, no overshoot was predicted for any of the Oatrim fluids considered in this study.

The startup results for $\dot{\gamma} = 10\ s^{-1}$ are illustrated in Fig. 5. The experimental results are qualitatively similar to the results at $\dot{\gamma} = 0.1\ s^{-1}$, with both the rise time to the maximum viscosity and the decrease to the steady value occurring at much shorter times at the higher shear rate. In this case, the Giesekus model overpredicts both the magnitude of the overshoot and the decay, although good qualitative agreement is still obtained. The K-BKZ model again underpredicts the overshoot, and the Bird–Carreau model rises monotonically to its final value. The most significant difference at the higher rate is that the prediction of the PTT model oscillates about its final value. The initial overshoot is captured very well at this shear rate, but instead of a single undershoot as at $\dot{\gamma} = 0.1\ s^{-1}$, the viscosity is predicted to oscillate with an amplitude that is initially ~20% of the steady value, and which decays slowly. A closed form for the steady-state viscosity was used to determine the ξ_i in Fig. 3, so the transient oscillation did not affect the fit. This oscillation is due to the fifth mode of the linear viscoelastic spectrum, so it is not a result of the large ξ_i in the other modes. Forcing ξ_5 to small values ($<10^{-3}$) can smooth the oscillations, but they are simply delayed to higher shear rates, while the steady value of the viscosity is increased. Although the parameter ϵ_i cannot be obtained from a fit to available experimental data, a value of $\epsilon_i = 0.1$ for each mode in Eq. (7) reduces the amplitude (and frequency) of oscillation, and the oscillations are damped much more quickly. Using the exponential form of Eq. (8) leads to even greater damping of the oscillations.

The stress relaxation modulus is shown in Fig. 6 as a function of time for strains from 0.02 to 2. For strains lower than 0.05, the stress relaxation modulus is independent of strain, indicating a region of linear viscoelastic behavior. This agrees well with the linear viscoelastic region determined from small amplitude oscillatory shear experiments, and as was shown in Fig. 2, the low strain stress relaxation data can be fitted with the same linear viscoelastic spectrum as the small amplitude oscillatory shear data. As the strain is increased, the value of the stress relaxation modulus decreases, but remains nearly parallel to the modulus at low strain. This justifies the assumption of time-strain separability in the K-BKZ model, and allows the damping function to be calculated. These values are

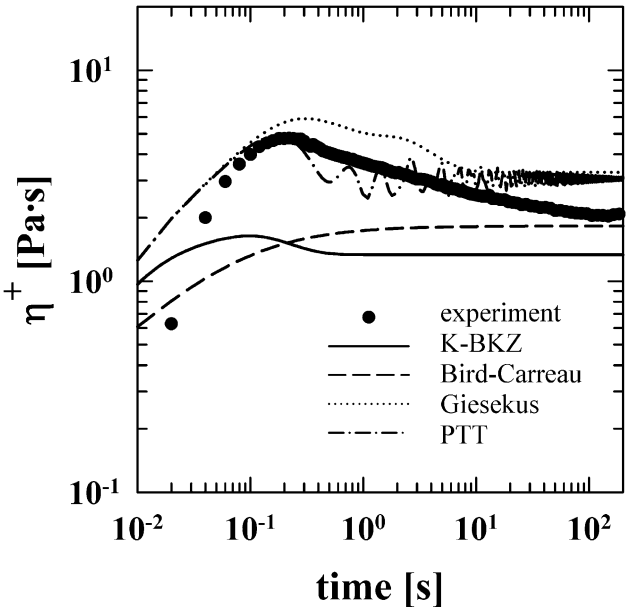

Fig. 5. Startup of steady shear flow of 12 wt% Oatrim-10 at $\dot{\gamma} = 10\ s^{-1}$.

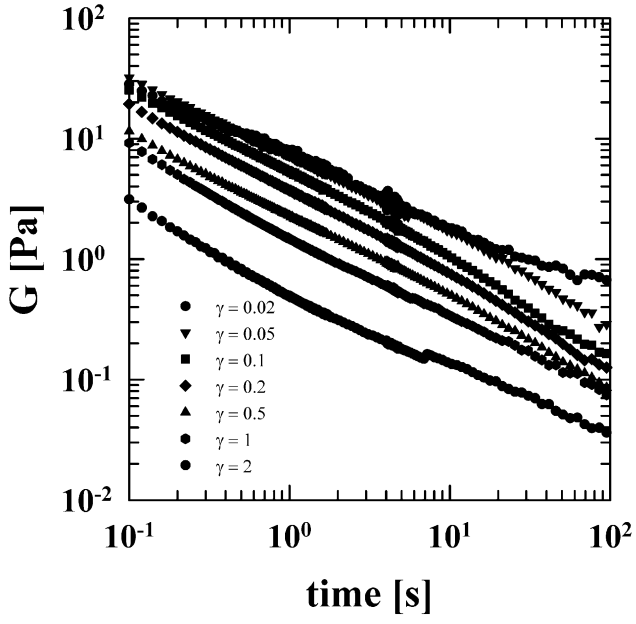

Fig. 6. Stress relaxation modulus of 12 wt% Oatrim-10.

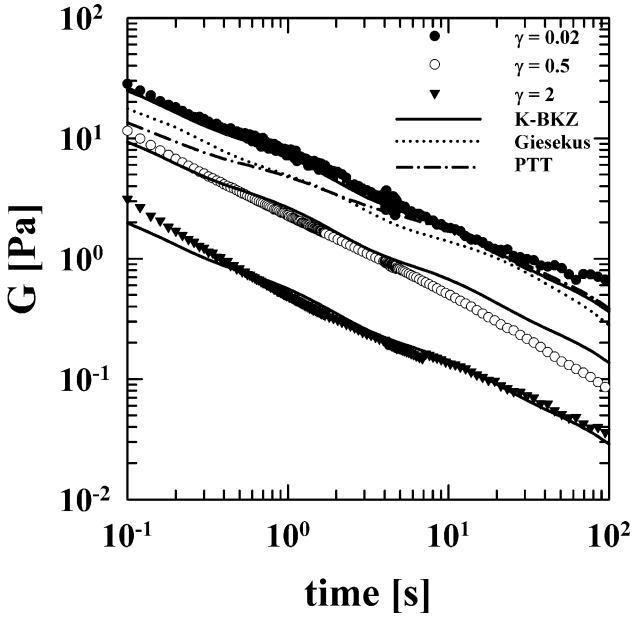

Fig. 7. Model predictions of stress relaxation modulus of 12 wt% Oatrim-10.

included in Table 1. As noted above, there is an upper limit on the concentration of Oatrim suspension that can be studied in shear flow due to slip at high concentrations when a gel begins to form. In contrast, there is a lower limit on the concentration for which stress relaxation data could be obtained due to the sensitivity of the rheometer. The 12 wt% Oatrim-10 suspension is therefore the focus of this work, since it was one of the few concentrations studied for which both steady shear and stress relaxation data could be obtained. Small amplitude oscillatory shear flow data were obtained for all concentrations.

Similar strain dependence was observed for the damping function for all of the high concentration suspensions. The damping functions for 15, 17.5 and 20 wt% Oatrim-5 suspensions were within 15% of each other over the range $0.01 \leq \gamma \leq 2$. The damping functions for Oatrim-10 suspensions decreased more sharply with strain, although they were within a factor of two of the Oatrim-5 suspensions at all strains.

The model predictions of the stress relaxation modulus are compared to the experimental results in Fig. 7, where results for only three strains are shown for clarity. The K-BKZ model accurately predicts the stress relaxation behavior over the entire range of strains, which is to be expected since the stress relaxation data were used to determine the model's nonlinear response in terms of the damping function. Both the Giesekus and PTT models fail to capture the strain dependence of the stress relaxation modulus. The experimental stress relaxation modulus decreases to 3% of its initial value as the strain is increased from 0.02 to 2.0, but the models predict a decrease to only about 70%. Carriere et al. (2002) showed that the stress relaxation modulus flour suspensions also had very strong strain dependence. This is a special difficulty for the models raised by biopolymer systems, as they have been shown to be accurate in other systems. Holz, Fischer and Rehage (1999) showed the Giesekus model could accurately predict the stress relaxation behavior of the surfactant system cetyltrimethylammonium bromide–sodium salicylate (CTAB-NaSal). In that case, the stress relaxation modulus decreased to about 5% of its initial value for strains between 1 and 12. No results for the Bird–Carreau model are shown in Fig. 7. It is straightforward to impose an instantaneous strain for the K-BKZ model by means of the damping function. Stress relaxation predictions for the Giesekus and PTT models were calculated by first solving for the stress growth from rest at a given shear rate for a time $t = \gamma/\dot{\gamma}$. For $\dot{\gamma} \geq 10^8\ s^{-1}$, the stress at the end of the imposed strain was independent of the shear rate, and the resulting stresses were used as initial values for the stress relaxation with $\dot{\gamma} = 0$. However, for the Bird–Carreau model, the stress decreases with increasing strain rate, and the instantaneous application of a step strain cannot be approximated in this manner.

Suspensions with concentrations higher than 12 wt% for Oatrim-10 or 15 wt% for Oatrim-5 could not be characterized in steady shear flow or startup of shear flow because the samples slipped in the rheometer. However, these samples formed gels that were sufficiently strong that cylindrical samples could be molded and tested in biaxial extension, a compressional flow which requires slip at the contact surfaces. As seen from Eq. (1), when the test is performed with a constant velocity of the upper disk, the strain rate increases throughout the test. Furthermore, changing either the initial sample height or the velocity results in a different strain rate profile for the test.

Tests with different initial sample heights showed that the maximum stress that could be achieved before sample breakdown increased with decreasing initial sample height, until reaching a nearly constant value for initial heights less than 2.1 mm. Christianson, Casiraghi and Bagley (1985) showed the same dependence on sample height for wheat starch gels. The results below are truncated at the time when the stress reaches its maximum for each run. In order to check for sample fracture, tests were run with different maximum strains both below and above the strain for which the maximum stress was observed. Even for the higher strains, if the test was run and the upper plate was immediately lifted, the sample would return to its original dimensions, with no visible cracks or breaks on the sample surface. In all cases, the sample diameter was less than the upper disk diameter at the truncation time, and the maximum strain $\Delta h/h$ was 1.1, 2.2 and 2.3 for speeds of 0.1, 0.3 and 1.0 mm/s, respectively.

During the test, the edges of the samples appeared to remain parallel, indicating slip at the contact surfaces. However, for the very thin samples used here and the short test duration (<1 s at the highest speeds), visual inspection was not sufficient to ensure that slip was achieved. A more accurate determination of the effectiveness of the lubricants

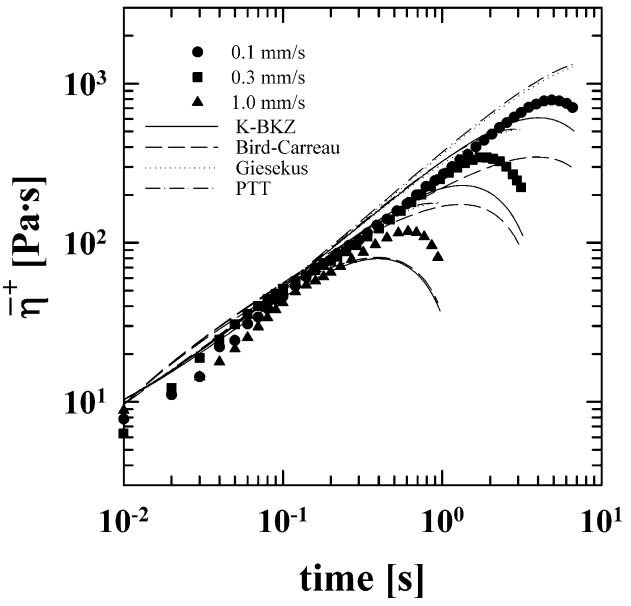

Fig. 8. Extensional stress growth coefficient in biaxial extension of 20 wt% Oatrim-5.

was obtained using the method of Mooney–Rivlin plots discussed by Bagley Christianson, and Wolf (1985). The quantity $\phi = f/(\lambda - \lambda^{-2})$ was plotted as a function of λ^{-1}, where f is the force per unit area of the unstrained sample and λ is the compression ratio. Vegetable oil, mineral oil and silicone oils were tested as lubricants. In each case, at $\lambda^{-1} > 1.1$, ϕ remained nearly constant at $\sim$95 Pa, until decreasing for $\lambda^{-1} > 2$. For plates with unlubricated teflon coating, ϕ increased to almost twice its plateau value at $\lambda^{-1} = 1.14$ before decreasing. Each of the lubricants improved the low-strain response both by decreasing the maximum value of ϕ and by decreasing the amount of compression required before reaching the constant value. The most effective lubricant was the vegetable oil, which produced constant ϕ values for $\lambda^{-1} \geq 1.04$.

The results for the biaxial extension of the 20 wt% Oatrim-5 gels are shown in Fig. 8 for upper plate speeds of 0.1, 0.3 and 1.0 mm/s. The maximum magnitude of the strain rate during each test was 0.16, 0.71 and 2.45 s^{-1}, respectively. The extensional stress growth coefficient, $\bar{\eta}^+ = \tau(t)/\dot{\epsilon}(t)$, is shown as a function of time for each velocity. At short times (t $\leq$ 0.5 s), the results superimpose for each velocity, but at longer times the extensional stress growth coefficient for the higher velocities decreases. The decrease is due both to the fact that the stress grows more slowly as it approaches its maximum value and to the fact that the magnitude of the strain rate increases as the sample height decreases. The results at short time are very sensitive to the value of the initial sample height determined from the results, but for $t \geq 0.3$ s, duplicate runs at a given velocity agree within 15%.

The predictions of each of the models are also shown in Fig. 8. Small amplitude oscillatory shear and low strain stress relaxation experiments were used as above to determine the linear viscoelastic spectrum, and stress relaxation experiments at high strains were used to determine the damping function for the K-BKZ model, and these results are given in Table 2. However, the other models require measurements of the viscosity to determine their nonlinear parameters, and the viscosity could not be measured due to slip for this sample. In order to study the qualitative response of the other models, the calculations in Fig. 8 are based on estimated values of the nonlinear parameters given in Table 2. The corresponding velocity for each curve can be obtained from Fig. 8 by noting that for each velocity the calculations were truncated at the same time as the experimental data.

At short times, all of the models predict similar results, and they all agree well with the experimental data. This indicates that the extensional stress growth follows linear viscoelastic behavior for the majority of each run, and that the linear viscoelastic spectrum obtained from shear flow measurements also describes the flow behavior in extension. The models differ, however, in their predictions near the end of each run as the strain rate increases. The Giesekus and PTT models fail to predict the downturn in $\bar{\eta}^+$ at longer times. The predicted stress continues to increase for these models, but $\bar{\eta}^+$ increases less rapidly at the end of each run when the strain rate increases sharply. In contrast, the predicted stress for the K-BKZ and Bird–Carreau models approaches a constant value, so that a higher strain rate results in a lower extensional stress growth coefficient. Although the results in Fig. 8 are for a transient flow, the model predictions can also be understood in terms of the steady-state predictions of the

Table 2
Model parameters for the 20 wt% Oatrim-5 sample

	λ_i (s)	η_i (Pa s)	Giesekus	PTT		K-BKZ		Bird–Carreau	
			α_i	ξ_i	ϵ_1	K	a_i	λ_i (s)	α_i
1	0.01	2.45	0.1	0.2	0.4	0.17	0.034	300	3.0
2	0.1	2.99	0.1	0.2	0.4		0.01	700	3.3
3	1	26.5	0.1	0.2	0.4				
4	10	229	0.1	0.2	0.4				
5	100	4140	0.1	0.2	0.4				
6	1000	44,600	0.1	0.2	0.4				

extensional viscosity. The K-BKZ, Bird–Carreau and PTT models all predict a strain-thinning extensional viscosity, so the stress is expected to increase more slowly as the strain rate increases. However, the steady-state values predicted by the K-BKZ and Bird–Carreau models are much lower than for the PTT model, and the steady value is reached more quickly for the integral models. Because the transient prediction for the PTT model is still well below the steady-state value for the time scale of the experiment, the fact that the steady value exhibits strain-thinning is not expected to be apparent in the transient calculations of Fig. 8. For the same reason, the predictions of the Giesekus and PTT models are nearly independent of the values of the nonlinear parameters used. While the nonlinear parameters affect the steady-state values of the extensional viscosity, they have little effect on the transient stress growth at short times. In contrast, all of the parameters for the Bird–Carreau model had to be selected within narrow ranges to obtain the predictions in Fig. 8.

4. Conclusions

The predictions of the K-BKZ, Giesekus, Phan-Thien–Tanner and Bird–Carreau constitutive models were compared to the flow behavior of Oatrim suspensions in a range of flows. At low concentrations, the β-glucan/amylodextrin blends formed shear-thinning suspensions. As the concentration was increased, an increasingly strong gel was formed, until eventually slip was observed in shear flow. The model parameters were determined from small amplitude oscillatory shear flow and the viscosity for the PTT, Giesekus and Bird–Carreau models, and from small amplitude oscillatory shear flow and stress relaxation for the K-BKZ model. While each of the models was versatile enough to fit a single flow well, they varied in their ability to predict other flows.

The Giesekus and PTT models both predicted the stress growth on startup of steady shear well, although the PTT model predicted an oscillating stress at high shear rates. This would not necessarily limit the model's use in solving flow problems, since the high Deborah number would impose a much more severe limitation on current numerical algorithms. The K-BKZ model gave qualitatively accurate results, although it underpredicted the stress overshoots. The Bird–Carreau model failed to predict either an overshoot or the correct time to reach a steady value.

The stress relaxation modulus showed very strong strain dependence, and this could only be modeled by the K-BKZ equation. The double exponential damping function used was general enough to incorporate the large changes in the stress relaxation modulus. The fluids studied showed time-strain separability, so the K-BKZ equation was well-suited for modeling this flow. The Giesekus and PTT models both predicted small decreases in the stress relaxation modulus with increasing strain, but they could not predict the stress relaxation modulus accurately at large strain. Because the stress in the Bird–Carreau model is defined in terms of an integral over past strain rates, the instantaneous imposition of a step strain could not be defined for this model.

In biaxial extension, all of the models gave accurate results at short times when the response was in the linear region, but they deviated at larger times as the strain increased. None of the models gave quantitative agreement with the experimental results at longer times, but the K-BKZ and Bird–Carreau models predicted an approach to a constant stress as was observed experimentally.

The nature of the Oatrim suspensions may limit the extension of the current results to other temperatures. As the temperature changes, the solubility of the β-glucan and amylodextrin components of the Oatrim suspension will change. As a result, the relaxation times of the linear viscoelastic spectrum may not all have the same temperature dependence. Carriere and Inglett (1999) concluded that interactions between the components caused the shear-thickening of the viscosity at intermediate shear rates. As the temperature was increased, the shear-thickening disappeared, although the shear rate dependence of the viscosity at other shear rates remained similar. Calculations at other temperatures therefore may require further rheological measurements to determine the linear and nonlinear model parameters.

Although Section 2.3 described the motivation behind the derivation of the Giesekus and PTT models, it should be noted that the nonlinear parameters for these models were obtained from fitting experimental data, and not from molecular details of the fluid. The Oatrim suspensions studied here are not expected necessarily to follow reptation (Giesekus) or network (PTT) behavior. The extreme values of the nonlinear parameters required to fit the shear rate dependence of the viscosity further show that the model parameters cannot be interpreted to understand the detailed structure of the fluid. Nevertheless, the mathematical form of each equation allows accurate prediction of the Oatrim suspension rheological properties. The K-BKZ and Bird–Carreau models are both empirical models, and no physical interpretation of their nonlinear parameters is assumed in their derivation.

The flows studied here tested a wide range of the fluid responses, and served to demonstrate the differences between the models considered. The K-BKZ model gave the most accurate results overall, although the Giesekus or PTT models may be accurate enough in many cases. The Bird–Carreau model failed to capture many important features of the flow. For many processing applications, an accurate prediction of the viscosity is most important. All of the models can predict the shear-rate dependence of the viscosity, but the Giesekus and PTT models predicted the transient response upon a change in shear rate much better than the K-BKZ and Bird–Carreau models did. The differential models may therefore be most useful for

processing design. The use of these models for biopolymer solutions appears to be justified, although care must be taken in each case to ensure that the model performs well in a range of flows of interest. The Oatrim suspensions studied here raise special issues due to their long relaxation times, strong strain dependence of the stress relaxation modulus, and strain-thinning of the biaxial extensional viscosity.

Acknowledgements

The technical assistance of Steven A. Lyle is gratefully acknowledged. This work was supported financially by the United States Department of Agriculture, Agricultural Research Service.

References

Autio, K., Myllymäki, O., & Mälkki, Y. (1987). Flow properties of oat β-glucans. *Journal of Food Science*, *52*, 1364–1366.

Bagley, E. B. (1992). Constitutive models for doughs. In J. L. Kokini, C.-T. Ho, & M. V. Karwe (Eds.), *Food extrusion science and technology* (pp. 203–211). New York: Marcel Dekker.

Bagley, E. B., Christianson, D. D., & Wolf, W. J. (1985). Frictional effects in compressional deformation of gelatin and starch gels and comparison of material response in simple shear, torsion and lubricated uniaxial compression. *Journal of Rheology*, *29*, 103–108.

Bernstein, B., Kearsley, E. A., & Zapas, L. J. (1963). A theory of stress relaxation with finite strain. *Transactions of the Society of Rheology*, *7*, 391–410.

Bird, R. B., Armstrong, R. A., & Hassager, O. (1987). *Dynamics of polymeric liquids, volume 1: Fluid mechanics*. New York: Wiley.

Bird, R. B., & Carreau, P. J. (1968). A nonlinear viscoelastic model for polymer solutions and melts—I. *Chemical Engineering Science*, *23*, 427–434.

Carreau, P. J., MacDonald, I. F., & Bird, R. B. (1968). A nonlinear viscoelastic model for polymer solutions and melts—II. *Chemical Engineering Science*, *23*, 901–911.

Carriere, C. J., & Inglett, G. E. (1998). Solution viscoelastic properties of Oatrim-10 and cooked oat bran. *Cereal Chemistry*, *75*, 354–359.

Carriere, C. J., & Inglett, G. E. (1999). Nonlinear viscoelastic solution properties of oat-based β-glucan/amylodextrin blends. *Carbohydrate Polymers*, *40*, 9–16.

Carriere, C. J., Thomas, A. J., & Inglett, G. E. (2002). Prediction of the nonlinear transient and oscillatory rheological behavior of flour suspensions using a strain-separable integral constitutive equation. *Carbohydrate Polymers*, *47*, 219–231.

Chatraei, S., & Macosko, C. W. (1981). Lubricated squeezing flow: a new biaxial extensional rheometer. *Journal of Rheology*, *25*, 433–443.

Christianson, D. D., Casiraghi, E. M., & Bagley, E. B. (1985). Uniaxial compression of bonded and lubricated gels. *Journal of Rheology*, *29*, 671–684.

Dhanasekharan, M., Huang, H., & Kokini, J. L. (1999). Comparison of observed rheological properties of hard wheat flour dough with predictions of the Giesekus–Leonov, White–Metzner and Phan-Thien–Tanner models. *Journal of Texture Studies*, *30*, 603–623.

Dhanasekharan, M., Wang, C. F., & Kokini, J. L. (2001). Use of nonlinear differential viscoelastic models to predict the rheological properties of gluten dough. *Journal of Food Process Engineering*, *24*, 193–216.

Doublier, J.-L., & Wood, P. J. (1995). Rheological properties of aqueous solutions of (1 → 3)(1 → 4)-β-D-glucan from oats (*Avena sativa* L.). *Cereal Chemistry*, *72*, 335–340.

van Es, H. E., & Christensen, R. M. (1973). A critical test for a class of nonlinear constitutive equations. *Transactions of the Society of Rheology*, *17*, 325–330.

Food and Drug Administration (1997a). Oats and coronary heart disease. *Federal Register*, *62*, 3584–3601.

Food and Drug Administration (1997b). Soluble fiber from whole oats and risk of coronary heart disease. *Federal Register*, *62*, 15343–15344.

Giesekus, H. (1982). A simple constitutive equation for polymer fluids based on the concept of deformation-dependent tensorial mobility. *Journal of Non-Newtonian Fluid Mechanics*, *11*, 69–109.

Holz, T., Fischer, P., & Rehage, H. (1999). Shear relaxation in the nonlinear-viscoelastic regime of a Giesekus fluid. *Journal of Non-Newtonian Fluid Mechanics*, *88*, 133–148.

Inglett, G. E. (1993). Amylodextrins containing β-glucans from oat flours and bran. *Food Chemistry*, *47*, 133–136.

Kaye, A., (1962). College of Aeronautics. Cranfield, Note No. 134 1962.

Kokini, J. L. (1994). Predicting the rheology of food biopolymers using constitutive models. *Carbohydrate Polymers*, *25*, 319–329.

Larson, R. G. (1988). *Constitutive equations for polymer melts and solutions*. Boston: Butterworth.

Malkin, A. Y., & Masalova, I. (2001). From dynamic modulus via different relaxation spectra to relaxation and creep functions. *Rheologica Acta*, *40*, 261–271.

Phan-Thein, N. (1978). A nonlinear network viscoelastic model. *Journal of Rheology*, *22*, 259–283.

Phan-Thein, N., & Tanner, R. I. (1977). A new constitutive equation derived from network theory. *Journal of Non-Newtonian Fluid Mechanics*, *2*, 353–365.

Soskey, P. R., & Winter, H. H. (1985). Equibiaxial extension of two polymer melts: Polystyrene and low density polyethylene. *Journal of Rheology*, *29*, 493–517.

Wikström, K., Lindahl, L., Andersson, R., & Westerlund, E. (1994). Rheological studies of water-soluble (1 → 3),(1 → 4)-β-D-glucans from milling fractions of oat. *Journal of Food Science*, *59*, 1077–1080.

Yamamoto, M. (1971). Rate-dependent relaxation spectra and their determination. *Transactions of the Society of Rheology*, *15*, 331–344.

Zhang, D., Doehlert, D. C., & Moore, W. R. (1998). Rheological properties of (1 → 3)(1 → 4)-β-D-glucans from raw, roasted, and steamed oat groats. *Cereal Chemistry*, *75*, 433–438.